

## Gate voltage tuning of photo-responses in n-AlGaAs/GaAs/AlGaAs double-heterojunction

Takuya Kawazu<sup>a)</sup>

*National Institute for Materials Science, 1-2-1 Sengen, Tsukuba, Ibaraki 305-0047, Japan*

<sup>a)</sup> Author to whom correspondence should be addressed: KAWAZU.Takuya@nims.go.jp

We demonstrate that the gate voltage  $V_g$  tunes the Schottky photocurrent  $I_{SG}$  for the irradiation of two lights (Light A and B) in an n-AlGaAs/GaAs/AlGaAs double-heterojunction. Light A is a 975-nm-laser that illuminates the entire Schottky gate region at  $280\mu\text{W}/\text{mm}^2$ . Light B is a 670-nm-laser that locally illuminates the ungated region at  $0.4\mu\text{W}$ . When  $V_g = 0\text{V}$ , Light B doubles  $I_{SG}$  for Light A. At  $V_g = 87\text{mV}$ ,  $I_{SG}$  is generated only when both Light A and B are irradiated simultaneously, like the logical operation  $A \cap B$ . When  $V_g = 165\text{mV}$ ,  $I_{SG}$  is induced only for the illumination of Light A alone, like  $A \cap \bar{B}$ .

Because of their importance as infrared (IR) detectors, the IR photo-response of Schottky barrier diodes has been extensively studied for decades.<sup>1-13)</sup> A Schottky-barrier photodetector typically comprises a thin metal film on a semiconductor, creating a rectifying potential barrier at the interface. The photon energy of the detectable light is determined by the Schottky barrier and not by the bandgap energy of the semiconductor. Therefore, an appropriate combination of a metal and a semiconductor can potentially detect infrared photons in the energy range of 0.2–0.6 eV.<sup>4-6)</sup>

In previous papers,<sup>11,13)</sup> we investigated the photo-response of an n-AlGaAs/GaAs heterojunction to illumination on the Schottky gate region and the ungated region. Our findings showed that a lateral photocurrent is generated in the two-dimensional electron gas (2DEG) only when both regions are illuminated, like the logical operation  $A \cap B$ .<sup>11)</sup> We also examined the Schottky photocurrent and found that the photocurrent caused by illumination of the Schottky gate region is enhanced by illumination of the ungated region.<sup>13)</sup> In this brief paper, the influence of the gate bias on the photo-response of the double heterojunction is studied. We measure the Schottky photocurrent  $I_{SG}$  at different gate voltages  $V_g$  and demonstrate that the value of  $V_g$  tunes  $I_{SG}$  for the illumination on the Schottky gate region and the ungated region.

For our study, a selectively doped n-AlGaAs/GaAs/AlGaAs double-heterojunction was prepared on a semi-insulating GaAs (100) substrate by molecular beam epitaxy. A 500-nm-thick GaAs buffer layer was grown, followed by a 310-nm-thick superlattice layer (10 nm  $\text{Al}_{0.27}\text{Ga}_{0.73}\text{As}/2$  nm GaAs), a 15-nm-thick GaAs quantum well (QW), a 10-nm-thick non-doped AlGaAs spacer, an 80-nm-thick Si-doped AlGaAs layer, and a 10-nm-thick GaAs capping layer. The heterojunction wafer was processed into a Hall bar structure with a Schottky gate. The Schottky gate was fabricated by vacuum evaporation of Al with a thickness of about 100 nm. The sample was bonded with silver paste in a ceramic package with a gold coated surface. The details of the sample preparation are given in Refs. 11–13.

To illuminate the Schottky gate region, we used a 975-nm-laser beam with an excited power density of about  $280 \mu\text{W}/\text{mm}^2$  (Light A) as the IR light source, which illuminated the entire sample structure (Fig. 1). The 100-nm-thick aluminum Schottky gate is expected to reflect over 90% of the incident light (using the Fresnel formula, the reflectance is approximately 94%). However, since the photon energy of Light A is less than the band gap energy of GaAs and AlGaAs, interband absorption does not occur, and GaAs and AlGaAs crystals are nearly transparent to the incident light. Therefore, the laser beam propagates through the sample, reflects off the back surface, and reaches the Schottky junction interface (Fig. 1(a)). Thus, Light A is capable of exciting photoelectrons at the metal-semiconductor interface in the Schottky gate region, as well as inducing an intraband transition that excites 2D electrons from the QW (Fig. 1(b)).

To illuminate the ungated region, we used a 670-nm-laser beam with an excitation power of  $0.4 \mu\text{W}$  (Light B) as the light source (Fig. 2). Light B was focused by a microscope objective lens into a  $50 \mu\text{m}$  diameter spot, allowing for observation of

the sample surface and precise monitoring of the irradiation position. The irradiation position is approximately 1.4 mm away from the gate region. The photon energy of Light B (wave length 670 nm) is about 1.85 eV, which exceeds the bandgap of  $\text{Al}_{0.27}\text{Ga}_{0.73}\text{As}$  ( $\sim 1.78$  eV), the superlattice, and GaAs. Using the absorption coefficient of AlGaAs to that of GaAs with the energy shift of the bandgap difference,<sup>14,15</sup> it is roughly estimated that about 10% of the incident light is absorbed by the n-AlGaAs layer, 30% by the superlattice layer, and the rest by the GaAs buffer layer, apart from surface reflection.

The absorption in the n-AlGaAs layer generates electrons and holes, and the electrons (holes) move toward the QW (surface) ((i) in Fig.2(b)). The electrons are immediately redistributed uniformly in the QW due to the high conductivity of the 2DEG channel. In contrast, the holes accumulate at the surface, but many of them recombine with electrons in the QW, where the recombination process is accelerated by the band flattening resulting from their Coulomb potential. Although some of the accumulated holes at the surface may move in the in-plane direction, their travel distance is insignificant due to the low mobility of holes. Therefore, the absorption in the n-AlGaAs layer has little effect on the Schottky photocurrent occurring at a large distance.

In the photo-absorption of the superlattice layer ((ii) in Fig.2(b)), generated holes move toward the GaAs buffer and accumulate there, while electrons are attracted to the QW and is redistributed in the QW. In contrast to the holes at the surface, those in GaAs have a relatively high mobility ( $\sim 400 \text{ cm}^2/\text{Vs}$ ).<sup>15</sup> Moreover, the holes are separated from the electrons that recombine with them by a thick superlattice. Therefore, the accumulated holes diffuse in the in-plane direction over a long distance and then spread to the Schottky gate region.

In the photo-absorption of the GaAs buffer layer ((iii) in Fig.2(b)), most of the generated electrons and holes are recombined due to their insufficient spatial separation. A few electrons still accumulate at the interface between the superlattice and the GaAs buffer, and then thermally cross the superlattice barrier into the QW. The remaining holes in the GaAs buffer are unable to recombine and diffuse in the in-plane direction. However, since the contribution of this process ((iii) in Fig.2(b)) is expected to be relatively small, the previous process ((ii) in Fig.2(b)) is most important for the in-plane hole diffusion. Note that only the holes that diffuse in the in-plane direction and reach the gate region can affect the Schottky photocurrent.

Figure 3(a) shows the Schottky photocurrent  $I_{SG}$  from the source contact to the gate, when Light A and/or B are turned on or off. No gate voltage is applied. On the horizontal axis of Fig. 3(a), A, B, and A+B represent the irradiations of Light A, B, and both, respectively. The measurement setup is schematically illustrated in Fig. 3(b). When the sample is illuminated with Light A, the photocurrent  $I_{SG}$  is about 12 nA ( $\equiv I_0$ ). In contrast, the photocurrent is not generated by Light B ( $I_{SG} = 0$  nA). When both Light A and B are irradiated, the resulting  $I_{SG}$  is about  $2I_0$  ( $= 24$  nA); Light B doubles the  $I_{SG}$  caused by Light A. The magnitude of  $I_0$  is proportional to the intensity of Light A, whereas the amount of the photocurrent increase depends on Light B. In the

experiment, the intensity of Light B was adjusted to achieve a doubling of the increase amount. The inset in Fig. 3(a) shows the summary table of the photocurrent responses.

Figure 4(a) shows the Schottky photocurrent  $I_{SG}$  from the source contact to the gate, where a voltage  $V_g$  of about 87 mV is positively applied between the gate and the source (Fig. 4(b)). When either Light A or B illuminates the sample, no photocurrent is observed ( $I_{SG} = 0$  nA). However, the photocurrent  $I_{SG}$  flows from the source to the gate for the irradiation of both Light A and B, and its value is equal to  $I_0$  (= 12 nA). The inset in Fig. 4(a) shows the summary table of the photocurrent responses. Note that the summary table corresponds to the logical operation  $A \cap B$ .

Figure 5(a) shows the Schottky photocurrent  $-I_{SG}$  from the gate to the source contact, where a voltage  $V_g$  of about 165 mV is positively applied between the gate and the source (Fig. 5(b)). When the sample is illuminated with Light A, the photocurrent  $-I_{SG}$  flows from the gate to the source, and its value is equal to  $I_0$  (= 12 nA). In contrast, no photocurrent is generated for the irradiation of Light B alone and for the irradiation of both Light A and B ( $I_{SG} = 0$  nA). The inset in Fig. 5(a) shows the summary table of the photocurrent responses. It corresponds to the logical operation  $A \cap \bar{B}$ .

When the sample is illuminated with Light A, electrons are excited in both the Schottky metal and the QW in the double hetero-junction (Figs. 3–5(c)). Electrons excited in the Schottky metal transfer to the QW ( $T_F$ ), while electrons excited in the QW transfer to the Schottky metal ( $T_R$ ). Such electron transfer induces the photocurrent  $I_{SG}$ , where the direction and the magnitude of  $I_{SG}$  are determined by the relationship between  $T_F$  and  $T_R$ .

More specifically,  $T_F$  is defined as the number of electrons per unit time that are photoexcited in the metal gate, overcome the Schottky barrier, and travel to the QW. The height of the Schottky barrier is reduced by the image-force lowering effect, the magnitude of which is proportional to the square of the electric field on the semiconductor side of the Schottky metal-semiconductor interface.<sup>16)</sup> Even if the electrons overcome the barrier, some electrons may not reach the QW due to scattering processes, and the probability of their arrival increases with increasing electric field from the QW to the Schottky gate. Therefore, the electric field in the sample is of great importance and significantly affects the value of  $T_F$ . Similarly,  $T_R$  is defined as the number of electrons per unit time that are photoexcited in the QW, travel to the Schottky barrier, and cross it. As in the case of  $T_F$ , the electric field within the sample influences the height of the Schottky barrier and the probability of the electron arrival.

The irradiation of Light B alone does not generate the photocurrent, as shown at B in Figs. 3–5(a). When the sample is irradiated with Light B, electrons and holes are excited in the 310-nm-thick superlattice layer ((ii) in Fig. 2(b), Figs. 3–5(b)). While the electrons are attracted to the QW, the holes move toward the GaAs buffer, and then diffuse and spread to the Schottky

gate region. The positive charge of holes induces electric fields, promoting the electron transfer from the gate to the QW ( $T_F$ ) and inhibiting the electron transfer from the QW to the gate ( $T_R$ ).

The gate bias  $V_g$  plays a similar but opposite role to Light B. Applying the gate bias alone does not generate a current (off in Figs. 4(a) and 5(a)). However, the positive gate bias induces the electric field directed from the Schottky metal gate to the QW. Since the traveling electrons are subjected to the electric field, the electron transfer from the QW to the gate ( $T_R$ ) increases and from the gate to the QW ( $T_F$ ) decreases. Note that applying the gate bias promotes  $T_R$ , while irradiating Light B promotes  $T_F$ .

When Light A illuminates the sample and no gate bias is applied, the electron transfer from the gate to the QW ( $T_F$ ) is larger than that ( $T_R$ ) from the QW to the gate (Fig. 3(c)), resulting in a net current  $I_{SG}$  of 12 nA ( $\equiv I_0$ ) (A in Fig. 3(a)). The irradiation of Light B increases  $T_F$  and decreases  $T_R$ . Therefore, Light B amplifies  $I_{SG}$  caused by Light A, resulting in a doubling of  $I_{SG}$  to  $2I_0$  (A+B in Fig. 3(a)).

As the gate bias  $V_g$  increases, the electron transfer  $T_F$  ( $T_R$ ) for the irradiation of Light A decreases (increases). At  $V_g = 87$  mV,  $T_F$  is equal to  $T_R$ , resulting in a net current of zero ( $I_{SG} = 0$  A at A in Fig. 4(a)). When Light B is irradiated,  $T_F$  increases and  $T_R$  decreases, leading to the generation of the photocurrent  $I_{SG} = I_0$ , as shown at A+B in Fig. 4(a).

With a further increase in the gate bias  $V_g$ , the electron transfer  $T_F$  is smaller than  $T_R$  for the irradiation of Light A (Fig. 5(c)). Consequently, the photocurrent  $-I_{SG}$  flows from the Schottky metal gate to the source contact (Fig. 5(b)). At  $V_g = 165$  mV,  $-I_{SG}$  is about  $I_0$ , as shown at A in Fig. 5(a). When Light B is irradiated,  $T_F$  increases and  $T_R$  decreases, resulting in  $T_F = T_R$  and, therefore,  $I_{SG} = 0$  A (A+B in Fig. 5(a)).

Although qualitative explanations of the experimental results have been provided, a deeper understanding of the phenomenon would require a more comprehensive investigation. In particular, it is necessary to study quantitatively how the transfer rates  $T_F$  and  $T_R$  are affected by the image force lowering effect and the probability of electron arrival. Such a quantitative analysis can be performed by examining the dependence of the Schottky photocurrent on the wavelength of the incident light, which is currently under investigation.

In this work, we demonstrated that the Schottky photocurrent signal behaves in a manner analogous to logical operations. Optically controlled switching and logic devices are considered essential technologies for optical computing and digital communication systems.<sup>17)-22)</sup> Previously, it was shown that an n-p-n-p Shockley diode with a QW can operate as an optical logic device that changes its logic function depending on the applied voltage.<sup>20,22)</sup> However, Shockley diodes, originally developed as thyristors, need a reset process to switch from ON state back to OFF state. An optical logic device has also been proposed, consisting of two heterojunction phototransistors sensitive to two different wavelengths, which does not require a reset process.<sup>21)</sup> But, the logic function is limited to the AND operation. The advantage of our method is that no reset process

This is the author's peer reviewed, accepted manuscript. However, the online version of record will be different from this version once it has been copyedited and typeset.

PLEASE CITE THIS ARTICLE AS DOI: 10.1063/1.50233346

is required and the logic operations ( $A \cap B$ ,  $A \cap \bar{B}$ ) are switched by the applied bias. In addition, we use two different types of light absorption, one for the semiconductor bandgap and the other for the Schottky barrier. This differs from previous studies, which have utilized only the former type of absorption. Our approach potentially offers a wider choice of two light wavelengths. Moreover, two optical detections are performed at a distance from each other, allowing for a wider range of device designs. However, our result only showed the possibility of the logic device with optical input and electrical output, although all optical logic element (i.e., optical output) is plausible for practical applications. This issue is left for future work.

In summary, we have studied the Schottky photocurrent  $I_{SG}$  for the irradiation of two lights (Light A and B) in an n-AlGaAs/GaAs/AlGaAs double-heterojunction and demonstrated that the photo-responses are tuned by the gate bias  $V_g$ . Light A, a 975-nm-laser beam with an intensity of approximately  $280 \mu\text{W}/\text{mm}^2$ , illuminated the entire sample structure. Light B, a 670-nm-laser beam with an intensity of approximately  $0.4 \mu\text{W}$ , locally illuminated the ungated region of the sample structure. With no gate bias applied, the irradiation of Light A causes  $I_{SG}$  of about 12 nA ( $\equiv I_0$ ) from the source contact to the gate. Conversely, the photocurrent is not generated by the irradiation of Light B alone. If both Light A and B are irradiated, Light B amplifies  $I_{SG}$  for Light A by a factor of 2. When a gate bias  $V_g$  of 87 mV is applied, no photocurrent is observed for the irradiation of either Light A or B. Only the irradiation of both Light A and B causes  $I_{SG} (= I_0)$ , like the logical operation  $A \cap B$ . When  $V_g = 165$  mV, no photocurrent is generated for the irradiation of Light B alone and for the irradiation of both Light A and B. Only if Light A is irradiated alone,  $I_{SG} (= -I_0)$  is induced, like the logical operation  $A \cap \bar{B}$ .

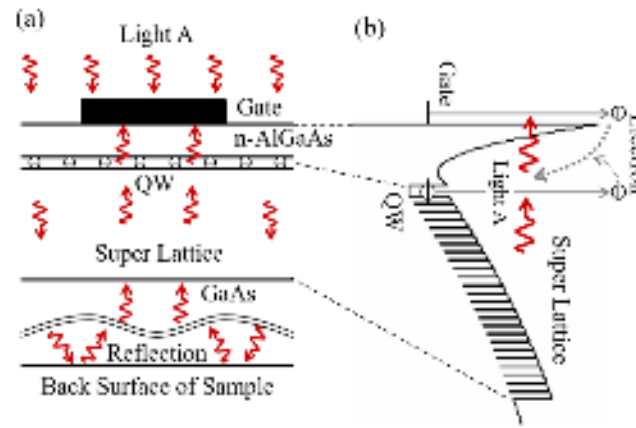


FIG. 1. Schematic drawings of the sample cross-section view (a) and the band diagram of n-AlGaAs/GaAs/AlGaAs double-heterojunction (b) when Light A is irradiated.

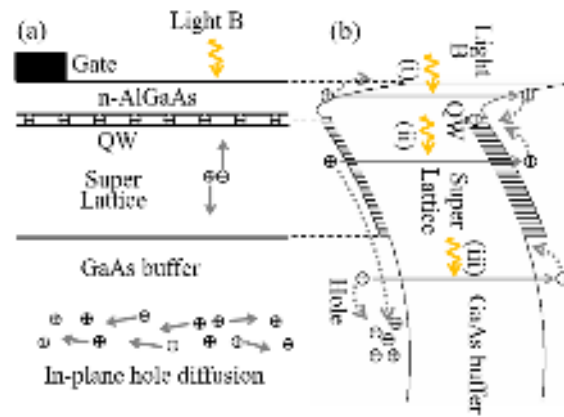


FIG. 2. Schematic drawings of the sample cross-section view (a) and the band diagram of n-AlGaAs/GaAs/AlGaAs double-heterojunction (b) when Light B is irradiated.

This is the author's peer reviewed, accepted manuscript. However, the online version of record will be different from this version once it has been copyedited and typeset.

PLEASE CITE THIS ARTICLE AS DOI: 10.1063/1.50233346

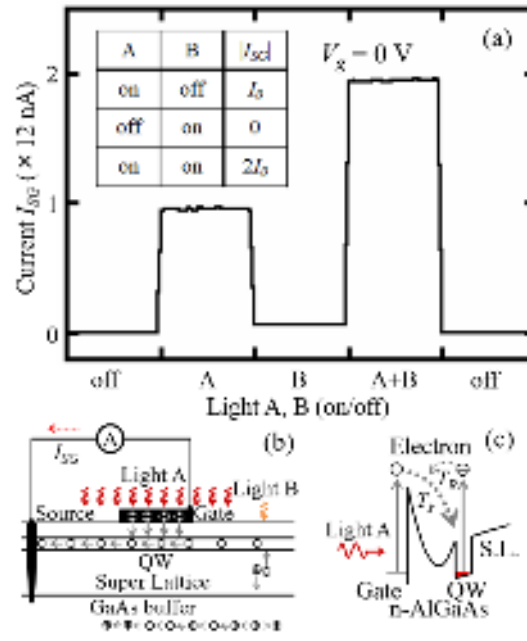


FIG. 3. Measured photocurrent  $I_{sg}$  for on/off action of Light A (975 nm) and B (670 nm) at the gate bias of  $V_g = 0$  V (a). Schematic drawings of the sample cross-section view (b) and the band diagram of n-AlGaAs/GaAs/AlGaAs double-heterojunction (c).

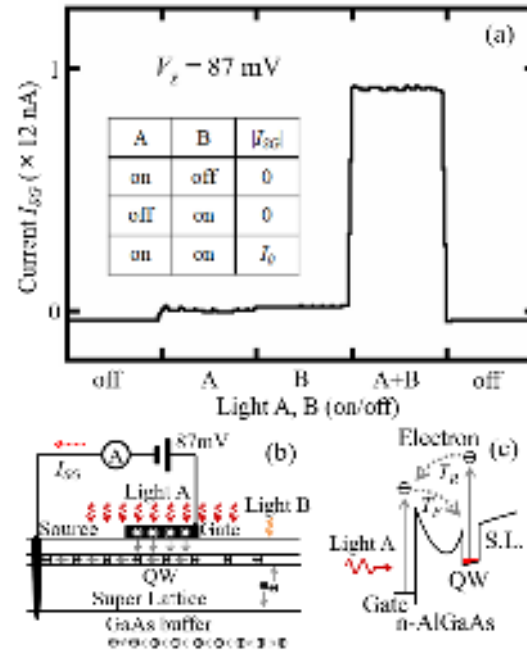


FIG. 4. Measured photocurrent  $I_{sg}$  for on/off action of Light A (975 nm) and B (670 nm) at the gate bias of  $V_g = 87$  mV (a). Schematic drawings of the sample cross-section view (b) and the band diagram of n-AlGaAs/GaAs/AlGaAs double-heterojunction (c).

This is the author's peer reviewed, accepted manuscript. However, the online version of record will be different from this version once it has been copyedited and typeset.

PLEASE CITE THIS ARTICLE AS DOI: 10.1063/1.5233346

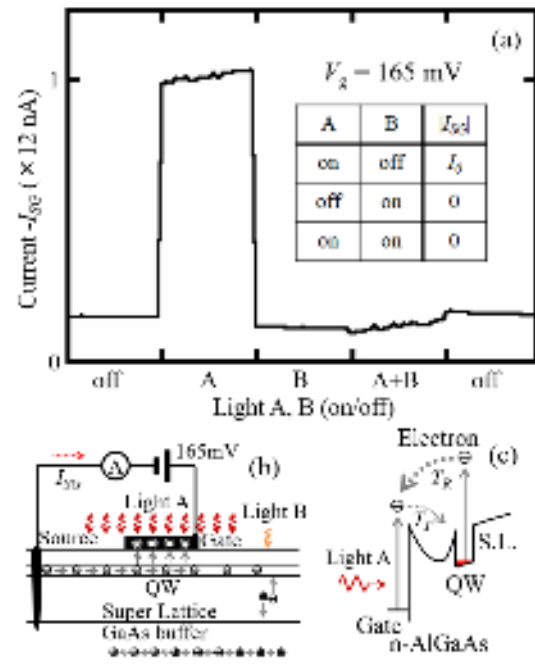


FIG. 5. Measured photocurrent  $I_{SG}$  for on/off action of Light A (975 nm) and B (670 nm) at the gate bias of  $V_g = 165$  mV (a). Schematic drawings of the sample cross-section view (b) and the band diagram of n-AlGaAs/GaAs/AlGaAs double-heterojunction (c).

## References

- 1) W. G. Spitzer, C. R. Crowell, and M. M. Atalla, *Phys. Rev. Lett.* **8**, 57 (1962).
- 2) M. Casalino, L. Sirleto, L. Moretti, and I. Rendina, *Semicond. Sci. Technol.* **23**, 075001 (2008).
- 3) S. Zhu, M. B. Yu, G. Q. Lo, and D. L. Kwong, *Appl. Phys. Lett.* **92**, 081103 (2008).
- 4) E. Elabd, T. Villani, and W. Kosonocky, *IEEE Electron Devices Lett.*, **3**, 89 (1982).
- 5) W. F. Kosonocky, F. W. Shallcross, T. S. Villani, and J. V. Groppe, *IEEE Trans. Electron Devices*, **32**, 1564 (1985).
- 6) C. K. Chen, B. Nechay, and B.-Y. Tsaur, *IEEE Trans. Electron Devices*, **38**, 1094 (1991).
- 7) A. Y. Tamera, A. Madjar, and P. R. Herezfeld, *IEEE Transactions on Microwave Theory and Techniques* **49**, 1900 (2001).
- 8) C. Scales and P. Berini, *IEEE J. Quantum Electron.* **46**, 633 (2010).
- 9) T. Kawazu, T. Noda, Y. Sakuma, and H. Sakaki, *Appl. Phys. Lett.* **106**, 022103 (2015).
- 10) T. Kawazu, T. Noda, and Y. Sakuma, *Jpn. J. Appl. Phys., Part 1* **56**, 04CG04 (2017).
- 11) T. Kawazu, T. Noda, and Y. Sakuma, *Appl. Phys. Lett.* **112**, 072101, (2018).
- 12) T. Kawazu, T. Noda, and Y. Sakuma, *Jpn. J. Appl. Phys.*, **58**, SIIB05 (2019).
- 13) T. Kawazu, *Jpn. J. Appl. Phys.*, **59**, 124003 (2020).
- 14) V. Swaminathan, P. J. Anthony, J. R. Pawlik, and W. T. Tsang, *J. Appl. Phys.* **54**, 2623 (1983).
- 15) *Data in Science and Technology, Semiconductors, Group IV elements and III-V Compounds*, edited by R. Poersschke, O. Madelung (Springer-Verlag, Berlin, 1991).
- 16) S. M. Sze, *Physics of Semiconductor Devices* (Wiley, New Jersey, 2007).
- 17) K. Matsuda, K. Takimoto, D. H. Lee, and J. Shibata, *IEEE Trans. Electron Devices* **37**, 1630 (1990).
- 18) K. Matsuda, H. Adachi, T. Chino, and J. Shibata, *IEEE Electron Device Lett.* **11**, 442 (1990).
- 19) W. K. Chan, J. P. Harbison, A. C. von Lehmen, L. T. Florez, C. K. Nguyen, and S. A. Schwarz, *Appl. Phys. Lett.* **58**, 2342 (1991).
- 20) M. S. Ünlü, S. Strite, A. Salvador, A. L. Demirel, and H. Morkoç, *IEEE Trans. Photon. Technol. Lett.* **3**, 1126 (1991).
- 21) X. An, K. M. Geib, M. J. Hafich, T. E. Crumbaker, P. Silvestre, F. R. Beyette, Jr., S. A. Feld, G. Y. Robinson, and C. W. Wilmsen, *Appl. Phys. Lett.* **61**, 636 (1992).
- 22) M. S. Ünlü, S. Strite, A. L. Demirel, S. Tagiran, A. Salvador, and H. Morkoç, *IEEE J. Quantum Electron.* **29**, 411 (1993).